

## Communications to the Editor

### How Do Oxidized Thiolate Ligands Affect the Electronic and Reactivity Properties of a Nitrile Hydratase Model Compound?

Irene Kung, Dirk Schweitzer, Jason Shearer,  
Wendy D. Taylor, Henry L. Jackson, Scott Lovell, and  
Julie A. Kovacs\*

Department of Chemistry, University of Washington  
Seattle, Washington 98195

Received May 22, 2000

Nitrile hydratases (NHase) are non-heme Fe(III)-containing, or noncorrinoid Co(III)-containing, microbial enzymes that catalyze nitrile hydration.<sup>1</sup> The iron form has been studied most extensively. The Fe(III) active site is low spin ( $S = 1/2$ ), and ligated by three cysteinates, two peptide amide nitrogens and either a hydroxide or an NO.<sup>2–4</sup> Given the high amount of sequence homology in the active site region, it is likely that the Co-NHase active site is virtually identical to Fe-NHase.<sup>1,5</sup> In one of two recent Fe NHase crystal structures<sup>2,4</sup> two of the metal-bound sulfurs appear to be oxidized, one to a sulfenate ( $^{114}\text{S}^{\text{cys}}=\text{O}$ ) and the other to a sulfinate ( $^{114}\text{S}^{\text{cys}}(=\text{O})_2$ ).<sup>4</sup> The sulfenate is not observed by mass spectrometry.<sup>6</sup> Sulfenic acids are usually unstable,<sup>7</sup> and metal–sulfenates are readily oxidized to metal–sulfinates.<sup>8,9</sup> A few synthetic NHase models containing oxidized sulfurs have been reported,<sup>10–12</sup> however, none of these incorporate a sulfenate, and only one<sup>12</sup> has an open coordination site.

Our group has shown that the spin-state and spectroscopic properties of Fe-NHase can be nicely reproduced by six-coordinate Fe(III) model complexes containing two cis-thiolates and imines.<sup>3,13–15</sup> These models lack oxidized sulfurs, yet their spectroscopic properties are remarkably similar to the enzyme, suggesting that two, of the three, cysteine NHase sulfurs remain unmodified. To understand how the sulfinate and, possibly, the

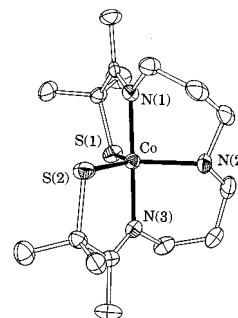


**Figure 1.** ORTEP plot of  $[\text{Co(III)}(\text{S}_2^{\text{Me}_2\text{N}_3(\text{Pr,Pr}))}]^+$  (**1**) showing 50% probability ellipsoids and the atom labeling scheme. H atoms have been omitted for clarity. Selected distances (Å) and angles (deg): Co–S(1), 2.162(2); Co–S(2), 2.158(2); Co–N(1), 1.923(4); Co–N(2), 2.060(5); Co–N(3), 1.923(4); S(1)–Co–S(2), 126.80(7); S(1)–Co–N(2), 117.3(1); S(2)–Co–N(2), 115.8(1).

sulfenate sulfur influences the electronic and reactivity properties of NHase, we have synthesized a series of sulfur-ligated, five-coordinate Co(III) model complexes containing progressively more oxidized sulfurs.

Five-coordinate  $[\text{Co(III)}(\text{S}_2^{\text{Me}_2\text{N}_3(\text{Pr,Pr}))}]^+$  (**1**) was synthesized in the same manner as its iron analogue.<sup>15</sup> Complex **1** is intermediate spin ( $S = 1$ ) over the temperature range 50–300 K (supplemental Figure S-1), and is reversibly reduced at  $E_{1/2} = -460$  mV vs SCE. The average Co–S distance (2.16(2) Å) in **1** (Figure 1)<sup>16</sup> is shorter than most Co(III) thiolates (average = 2.24 Å).<sup>17–19</sup> Azide and  $\text{SCN}^-$  bind quantitatively to **1** at room temperature trans to one of the thiolate sulfurs.<sup>20</sup>

Trigonal bipyramidal **1** ( $\tau = 0.87$ )<sup>21</sup> is converted to a more square pyramidal ( $\tau = 0.48$ ) sulfinate/thiolate-ligated complex,  $[\text{Co(III)}(\text{S}^{\text{Me}_2}(\text{S}^{\text{O}_2})\text{N}_3(\text{Pr,Pr}))]^+$  (**2**; Figure 2),<sup>22</sup> upon stirring in air for 3 days. Only one of the two thiolate sulfurs (S(2)) is oxidized, even upon prolonged stirring. Oxidation of S(2) causes the spin-state to change, from  $S = 1$  (in **1**) to 0 (in **2**), and the reduction potential to shift cathodically to  $E_{1/2} = -380$  mV vs SCE. The mean S(2)–O(1,2) distance (1.453(2) Å) in **2** falls in the usual range (1.42–1.48 Å).<sup>17,23,24</sup> The Co–S(2) distance in **2** is indistinguishable from Co–S(1) (Figure 2). Both of the Co–S bonds in **2** are slightly shorter than the Co–S bonds in **1**, because

(16) Crystallographic data (Mo K $\alpha$  ( $\lambda = 0.71073$  Å) radiation, Enraf-Nonius CAD4 diffractometer, 183 K) for **1** are as follows:  $\text{C}_{16}\text{H}_{31}\text{CoF}_6\text{N}_3\text{PS}_2$ , violet crystal, monoclinic, space group  $P2_1/n$ ,  $a = 12.042(2)$  Å,  $b = 14.661(3)$  Å,  $c = 13.795(2)$  Å,  $\beta = 109.90(2)^\circ$ ,  $V = 2290(1)$  Å<sup>3</sup>,  $Z = 4$ , 4588 observed reflections ( $I > 2.0\sigma(I)$ ),  $R = 0.0508$ ,  $R_w = 0.129$ . The structure was solved by direct methods using Siemens SHELXTL PLUS (PC version).

(17) This average, or range, was obtained from a search of the Cambridge crystallographic database.

(18) Beissel, T.; Glaser, T.; Kesting, F.; Wieghardt, K.; Nuber, B. *Inorg. Chem.* **1996**, *35*, 3936–3947.

(19) Fikar, R.; Koch, S. A.; Millar, M. M. *Inorg. Chem.* **1985**, *24*, 3311.

(20) Shearer, J.; Kung, I.; Kovacs, J. A. Manuscript in preparation.

(21)  $\tau$  is defined as  $(\alpha - \beta)/60^\circ$ , where  $\alpha =$  largest angle,  $\beta =$  second largest angle ( $\tau = 1.0$  for ideal trigonal bipyramidal;  $\tau = 0.0$  for ideal square pyramidal). Addison, A. W.; Rao, T. N.; Reedijk, J.; Van Rijn, J.; Verschoor, G. C. *J. Chem. Soc., Dalton Trans.* **1984**, 1349–1356.

(22) Crystallographic data (Mo K $\alpha$  ( $\lambda = 0.71070$  Å) radiation, Nonius Kappa CCD diffractometer, 161(2) K) for **2**:  $\text{C}_{16}\text{H}_{31}\text{F}_6\text{N}_3\text{O}_2\text{S}_2\text{Co}$ , magenta crystal, monoclinic space group  $P2_1/n$ ,  $a = 17.5681(5)$  Å,  $b = 11.4236(2)$  Å,  $c = 23.3285(8)$  Å,  $\beta = 96.583(1)^\circ$ ,  $V = 4650.9(2)$  Å<sup>3</sup>,  $Z = 8$ ; 13 388 observed reflections,  $R = 0.0658$ ,  $R_w = 0.1298$ , GOF = 1.04. The structure was solved by direct methods (SIR92) and refined with SHELX97.

(23) Grapperhaus, C. A.; Darendsbourg, M. Y. *Acc. Chem. Res.* **1998**, *31*, 451–459.

(24) Kumar, M.; Colpas, G. J.; Day, R. O.; Maroney, M. J. *J. Am. Chem. Soc.* **1989**, *111*, 8323–8325.

- (1) Kobayashi, M.; Shimizu, S. *Nature Biotechnol.* **1998**, *16*, 733–36.  
 (2) Huang, W.; Jia, J.; Cummings, J.; Nelson, M.; Schneider, G.; Lindqvist, Y. *Structure* **1997**, *5*, 691–699.  
 (3) Scarrow, R. C.; Strickler, B.; Ellison, J. J.; Shoner, S. C.; Kovacs, J. A.; Cummings, J. G.; Nelson, M. J. *J. Am. Chem. Soc.* **1998**, *120*, 9237–9245.  
 (4) Nagashima, S.; Nakasako, M.; Naoshi, D.; Tsujimura, M.; Takio, K.; Odaka, M.; Yohda, M.; Kamiya, N.; Endo, I. *Nature Struct. Biol.* **1998**, *5*, 347–351.  
 (5) Payne, M. S.; Wu, S.; Fallon, R. D.; Tudor, G.; Stieglitz, B.; Turner, I. M., Jr.; Nelson, M. J. *Biochemistry* **1997**, *36*, 5447–5454.  
 (6) Nojiri, M.; Yohda, M.; Odaka, M.; Matsushita, Y.; Tsujimura, M.; Yoshida, T.; Dohmae, N.; Takio, K.; Endo, I. *J. Biochem.* **1999**, *125*, 696–704.  
 (7) Claiborne, A.; Yeh, J. I.; Mallet, C.; Luba, J.; Crane, E. J.; Charrier, V.; Parsonage, D. *Biochemistry* **1999**, *38*, 15407–15416.  
 (8) Buonomo, R. M.; Font, I.; Maguire, M. J.; Reibenspies, J. H.; Tuntulani, T.; Darendsbourg, M. Y. *J. Am. Chem. Soc.* **1995**, *117*, 963–973.  
 (9) Adzamili, I. K.; Libson, K.; Lydon, J. D.; Elder, R. C.; Deutsch, E. *Inorg. Chem.* **1979**, *18*, 303–311.  
 (10) Tyler, L. A.; Noveron, J. C.; Olmstead, M. M.; Mascharak, P. K. *Inorg. Chem.* **2000**, *39*, 357–362.  
 (11) Tyler, L. A.; Noveron, J. C.; Olmstead, M. M.; Mascharak, P. K. *Inorg. Chem.* **1999**, *38*, 616–617.  
 (12) Heinrich, L.; Vaissermann, J.; Chottard, G.; Chottard, J.-C. *Angew. Chem., Int. Ed. Engl.* **1999**, *38*, 3526–3528.  
 (13) Schweitzer, D.; Ellison, J. J.; Shoner, S. C.; Lovell, S.; Kovacs, J. A. *J. Am. Chem. Soc.* **1998**, *120*, 10996–10997.  
 (14) Shoner, S. C.; Barnhart, D.; Kovacs, J. A. *Inorg. Chem.* **1995**, *34*, 4517–18.  
 (15) Ellison, J. J.; Nienstedt, A.; Shoner, S. C.; Barnhart, D.; Cowen, J. A.; Kovacs, J. A. *J. Am. Chem. Soc.* **1998**, *120*, 5691–5700.

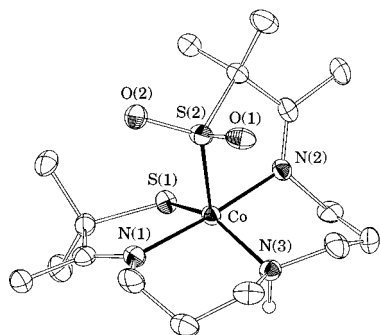


**Figure 2.** ORTEP plot of  $[\text{Co(III)}(\text{SMe}_2(\text{SO}_2)\text{N}_3(\text{Pr,Pr}))]^{2+}$  (**2**) showing 50% probability ellipsoids and the atom labeling scheme. All H atoms, except for the N–H proton, have been omitted for clarity. Only one of the two molecules contained in the asymmetric unit is shown. The second molecule is in a slightly different conformation ( $\tau = 0.56$ ).<sup>21</sup> Selected distances (Å) and angles (deg): Co–S(1), 2.121(1); Co–S(2), 2.116(1); Co–N(1), 1.938(3); Co–N(2), 1.913(3); Co–N(3), 2.026(3); S(2)–O(1), 1.451(3); S(2)–O(2), 1.455(3); S(1)–Co–S(2), 110.9(1); S(1)–Co–N(3), 145.7(1); N(1)–Co–N(2), 174.8(2).

the Co(III) ion of **2** is in a lower spin-state. The observed spin-state change is caused by the geometry change. The geometry change is most likely driven by the sulfinate ligand's preference for an apical site that lacks other ligands competing for overlap with the same  $p_z$  orbital. In contrast to bis-thiolate ligated **1**, sulfinate-ligated **2** does not bind  $\text{N}_3^-$  or  $\text{SCN}^-$  to its open coordination site. This reflects the stronger trans influence of sulfinate vs thiolate.<sup>9</sup>

Addition of  $\text{H}_2\text{O}_2$  to **2** results in the oxidation of the remaining thiolate to a sulfenate, and coordination of the added oxygen to the open binding site,<sup>25</sup> to form the  $\eta^2$ -bound sulfenate complex  $[\text{Co(III)}((\eta^2\text{-SO})(\text{SO}_2)\text{N}_3(\text{Pr,Pr}))]^{2+}$  (**3**).<sup>8,9</sup> No further oxidation of S(1) (Figure 3) is observed, even upon prolonged stirring with excess  $\text{H}_2\text{O}_2$ . The robust nature of the sulfenate in **3** is unusual,<sup>8,9</sup> and is probably due to its  $\eta^2$ -interaction with the metal. The only other example of an  $\eta^2$ -coordinated sulfenate is with V(V), an oxophilic metal ion.<sup>26</sup> Metal complexes incorporating both a sulfinate and sulfenate are extremely rare.<sup>8</sup> Complex **3** is diamagnetic, unreactive, and reduced at a more anodic potential ( $E_{1/2} = -775$  mV vs SCE) than are **1** and **2**. The S(1)–O(1) distance in **3** (Figure 3) falls in the usual range (1.50–1.60 Å)<sup>17</sup> for a sulfenate.<sup>9,23,26</sup> The longer Co–O(1) distance (usual range: 1.83–1.95 Å)<sup>17</sup> in **3** most likely reflects the more electrophilic nature of O(1). The Co–S(1) distance in **3** is slightly elongated (by 0.01 Å) relative to the corresponding distance in **2** and the

(25) Crystallographic data (Mo  $K\alpha$  ( $\lambda = 0.71070$  Å) radiation, Nonius Kappa CCD diffractometer, 161(2) K) for **3**:  $\text{C}_{16}\text{H}_{31}\text{F}_6\text{PN}_3\text{O}_5\text{S}_2\text{Co}$ , red crystal, monoclinic space group  $P2_1/c$ ,  $a = 11.2258(5)$  Å,  $b = 18.0951(9)$  Å,  $c = 12.1802(5)$  Å,  $\beta = 108.615(3)^\circ$ ,  $V = 2344.7(1)$  Å<sup>3</sup>,  $Z = 4$ ; 6622 observed reflections,  $R = 0.0564$ ,  $R_w = 0.1308$ , GOF = 0.950. The structure was solved by direct methods (SIR92) and refined with SHELX97.

(26) Commman, C. R.; Stautler, T. C.; Boyle, P. D. *J. Am. Chem. Soc.* **1997**, *119*, 5986–5987.

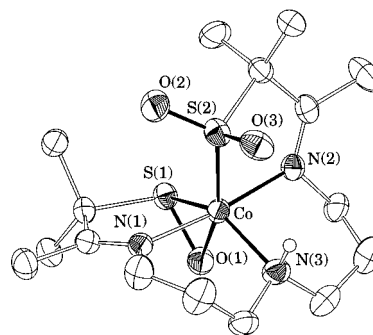


**Figure 3.** ORTEP plot of  $[\text{Co(III)}((\eta^2\text{-SO})(\text{SO}_2)\text{N}_3(\text{Pr,Pr}))]^{2+}$  (**3**) showing 50% probability ellipsoids and the atom labeling scheme. All H atoms, except for the N–H proton, have been omitted for clarity. Selected distances (Å) and angles (deg): Co–S(1), 2.132(1); Co–S(2), 2.118(1); Co–O(1), 2.042(2); Co–N(1), 1.957(3); Co–N(2), 1.943(3); Co–N(3), 1.993(3); S(1)–O(1), 1.548(3); S(2)–O(2), 1.454(3); S(2)–O(3), 1.464(3); S(1)–Co–S(2), 114.38(5); S(1)–Co–O(1), 43.5(1); S(1)–O(1)–Co, 71.4(1); S(1)–Co–N(3), 143.2(1); N(1)–Co–N(2), 173.6(1).

Co–S(2) in **3**, probably as a consequence of its  $\eta^2$ -binding mode. Coordination of the sulfenate oxygen in **3** does not appear to influence the trans Co–S(2) sulfinate interaction; the Co–S(2) distance is identical in **2** and **3**.

This work examines the influence that incremental oxidation of coordinated sulfur has on the reactivity and electronic properties of sulfur-ligated Co-NHase model compounds, and describes the first example of a model containing a sulfenate. The  $\eta^2$ -binding mode appears to prevent further oxidation of the sulfenate. The orientation of the sulfenate oxygen, syn to the open site, in the model described herein is identical to its orientation at the NHase active site.<sup>4</sup> In our model, however, this orientation results in the coordination of the oxygen, and this shuts down reactivity. The work reported herein therefore suggests that if the sulfenate  $\text{CysS}^{114}=\text{O}$  were present in the active form of NHase, it might interfere with reactivity, and therefore its function, by blocking the reactive site. It is also possible that the protein prevents  $\eta^2$ -coordination of  $\text{CysS}^{114}=\text{O}$ , by providing H-bonds (from several arg residues contained in the active site pocket) that stabilize the decoordinated form. This study also shows that the strong trans influence of a sulfinate will cause (1) the geometry to change so as to place the open site opposite the sulfinate, (2) the spin-state to change, (3) the Co(II) oxidation state to become more accessible, and (4) reactivity to decrease at the open site.

**Acknowledgment.** We thank Jerry A. Cowen for help with magnetic susceptibility measurements. Financial support from the NIH (Grant GM 45881) is also gratefully acknowledged.

**Supporting Information Available:** Detailed syntheses for **1**, **2**, and **3**, crystallographic data for **1**, **2**, and **3**, magnetic data ( $1/\chi$  vs  $T$  plot) for **1** (Figure S-1), and cyclic voltammograms for **1** (Figure S-2), **2** (Figure S-3), and **3** (Figure S-4) (PDF). This material is available free of charge via the Internet at <http://pubs.acs.org>.

JA0017561